Journal of Nuclear Materials 390–391 (2009) 355–358

Contents lists available at ScienceDirect

Journal of Nuclear Materials

journal homepage: www.elsevier.com/locate/jnucmat

Intermittent transport in the JET far-SOL

C. Silva [a,b,*], B. Gonçalves [a,b], C. Hidalgo [a,c], M.A. Pedrosa [a,c], W. Fundamenski [a,d], M. Stamp [a,d], R.A. Pitts [a,e], JET-EFDA contributors [1]

[a] JET-EFDA, Culham Science Centre, OX14 3DB, Abingdon, UK
[b] Associação Euratom/IST, Instituto de Plasmas e Fusão Nuclear, Instituto Superior Técnico, Portugal
[c] Associación Euratom/Ciemat, 28040 Madrid, Spain
[d] Euratom/UKAEA Association, Culham Science Centre, Abingdon, Oxon OX14 3DB, UK
[e] CRPP-EPFL, Lausanne 1015, Switzerland

ARTICLE INFO

PACS:
52.40.Hf
52.25.Fi
52.35.Ra

ABSTRACT

The intermittent transport in the JET scrape-off layer has been investigated using a multi-pin reciprocating Langmuir probe system. It was found that radial transport in the far-SOL is not continuous but occurs in short bursts observed most often at the beginning of each structure. The magnitude of the parallel ion flux during the filaments quickly decreases with radius, contrary to the cross-field velocity which has a weak radial dependence. Data from the JET boundary plasma have been analyzed to characterize the properties of the intermittent events. Statistical analysis reveals that the filament duration is larger on average in L-mode when compared to that observed during ELMs, while the radial velocity and the density perturbations are smaller.

1. Introduction

It is now widely accepted that intermittent convective transport, driven by radially propagating plasma structures, plays a pivotal role in determining the rate of cross-field particle and heat transport in the scrape-off layer (SOL). Intermittent events are field-aligned coherent structures propagating radially far into the SOL and have been observed in nearly all magnetically confined plasmas [1–5]. The distribution of the intermittent fluctuations deviates from Gaussian as filaments consist mainly of positive density bursts. Convective transport seems to be particularly important in the far-SOL plasma (outer midplane separatrix distance larger than ~3 cm) where it dominates over diffusive-like processes. These non-diffusive events transport particles radially to remote regions, with implications for main chamber plasma-facing components (PFCs), both in terms of deposited power and impurity production.

The main objective of this work is therefore to study intermittent events in the JET far-SOL, concentrating on the filamentary structure observed during ELMs, L-mode and in the inter-ELM phase. The structure of the large filaments observed during ELMs is investigated in detail as well as the ELM radial transport across the SOL. Furthermore, probe data from the JET boundary plasma have been analyzed to characterize the properties of the intermittent events and to obtain quantitative information on the size, duration and velocity associated with plasma structures.

2. Experimental results

The principal diagnostic used in this work is a 9-pin probe head mounted on a fast reciprocating drive system that inserts the probe into the plasma vertically at the top low field side of the plasma poloidal cross-section [6]. This allows the simultaneous measurement of the ion saturation current, I_{sat}, floating potential, V_f, electron temperature, T_e, and turbulent driven particle flux with a high temporal resolution (500 kHz). The cross-field fluctuations induced particle flux is estimated using $\Gamma_{E\times B} = \langle \tilde{n}\tilde{E}_\theta \rangle / B$, where $\tilde{n}$ and $\tilde{E}_\theta$ are the density and the poloidal electric field fluctuations, respectively. Density and plasma potential fluctuations are evaluated from I_{sat} and V_f, respectively, neglecting electron temperature fluctuations effects. Owing the high energy fluxes associated with many ELMs, their study with the JET probe is restricted to Type III ELMs in the main SOL, with measurements during Type I ELMs being possible only in the far-SOL.

2.1. Intermittent transport during ELMs

High temporal resolution measurements reveal that the ELM has a complex internal structure, being composed of a number of filaments [6–10]. Fig. 1 provides an illustration, showing the time

* Corresponding author. Address: Associação Euratom/IST, Instituto de Plasmas e Fusão Nuclear, Instituto Superior Técnico, Portugal.
E-mail address: csilva@ipfn.ist.utl.pt (C. Silva).

[1] See the Appendix of M.L. Watkins et al., Fusion Energy 2006 (Proc. 21st Int. Conf. Chengdu) IAEA (2006).

0022-3115/$ - see front matter © 2009 Elsevier B.V. All rights reserved.
doi:10.1016/j.jnucmat.2009.01.068

evolution of the parallel ion flux, J_{sat}, the radial velocity, v_r, and the time integrated turbulent particle flux during a small Type I ELM event ($\Delta W \sim 50$ kJ) measured at $r - r_{sep} \approx 4$ cm (#58641). The effective radial velocity has been defined as $\Gamma_{E\times B}$ normalized to the local density, $v_r = \langle \tilde{I}_{sat}\tilde{E}_\theta \rangle / \bar{I}_{sat}B$. Probe signals clearly show that the ELM event is composed of a number of sub-structures, which are also detected by other diagnostics such as the fast visible camera [11]. As shown by the shadowed area in Fig. 1, that indicates the time when the magnetic activity is significant, ELM filaments last for much longer than the MHD phase of the ELM. These well defined blobs-like structures are characterized by large density perturbations, up to twenty times the background (inter-ELM) value, propagating radially with velocities up to 1 km/s and lifetimes in the range 40–100 μs (as seen by the probe J_{sat}). The radial velocity corresponds to roughly 0.3% of the pedestal sound speed ($T_e^{ped} \approx T_i^{ped} \approx 1$ keV), in reasonable agreement with results obtained with the JET outerboard limiter probes, $v_r/c_s \sim 0.2\%$ [12]. Typically, 8–10 large filaments (J_{sat} perturbations larger than 1.5 times the background value) are observed per ELM separated in time by 50–400 μs. Because only a modest T_e rise is observed to be associated with them in the far-SOL, they are not responsible for any significant electron heat convection [6]. Filaments are also observed in Type III ELMs, being, however, its number, density perturbation and radial velocity smaller. For instance, for 300 Hz Type III ELMs, the number of filaments is limited to 2–3 and the radial velocity to 500 m/s.

As illustrated by the sharp increase in the time integrated $\Gamma_{E\times B}$, the radial transport in the SOL during ELMs is not continuous but occurs in short bursts, usually observed at the beginning of each event. This behaviour is more clearly seen in Fig. 2, which shows, on an expanded time scale, the evolution of J_{sat} and $\Gamma_{E\times B}$ during three filaments inside the ELM presented in Fig. 1. A substructure inside each individual filament is found, which differs from filament to filament, and is often observed to be double-peaked. Furthermore, signals from probe tips poloidaly separated by 1.4 cm reveal significant differences, showing that the filament is in fact a complex spatial structure. The observed behaviour is consistent with a model of radial blob transport in the SOL [13], which predicts that a symmetric blob structure develops into the shape of a mushroom-like cap, characterized by a sharp front and a trailing wake, and later to the breaking-up of the individual filaments. Measurements of the filaments crossing the probe are therefore expected to have a complex time behaviour.

Fig. 3 shows the radial profile of the ELM averaged J_{sat}, $\Gamma_{E\times B}$ and v_r for the same pulse shown in Fig. 1. The amplitude of both J_{sat} and $\Gamma_{E\times B}$ quickly decreases with radius in contrast to the trend observed for v_r, which has a weak radial dependence. Similar behaviour is observed in the instantaneous v_r measured during the ELM filaments. Although instantaneous radial velocities of 1 km/s are observed, the ELM averaged velocity is significantly smaller, <100 m/s. In contrast with the results reported here, DIII-D data shows that filaments slow down quickly with radius [2].

2.2. Intermittent transport in L-mode and in between ELMs

L-mode intermittent transport has been studied in great detail in the edge of tokamak plasmas [1–5]. The statistical properties of the SOL parameters show a deviation from the Gaussian distribution, featuring a positive skewness and kurtosis. Fig. 4 illustrates the time evolution of J_{sat}, v_r, and the time integrated $\Gamma_{E\times B}$ in an L-mode discharge at $r - r_{sep} \approx 2.5$ cm. Positive excursions of roughly two times the average density are observed, leading to transient particle transport. The amplitude of both J_{sat} and v_r in L-mode filaments is, however, significantly lower than that obtained during ELM. Intermittent events are also observed in the inter-ELM periods, Fig. 5. In this case, the amplitudes of J_{sat} and v_r excursions are even lower than in L-mode phase.

Conditional averaging of fluctuations in J_{sat}, $\Gamma_{E\times B}$ and v_r has been compared in L- and H-mode (both during small ELMs, $f_{ELM} \approx 100$ Hz, and in between ELMs) at $r - r_{sep} \approx 4$ cm. Fluctuations exceeding the mean J_{sat} by twice the standard deviation were selected and averaged, producing the results shown in Fig. 6. Results are also summarized in Table 1, which shows the filaments

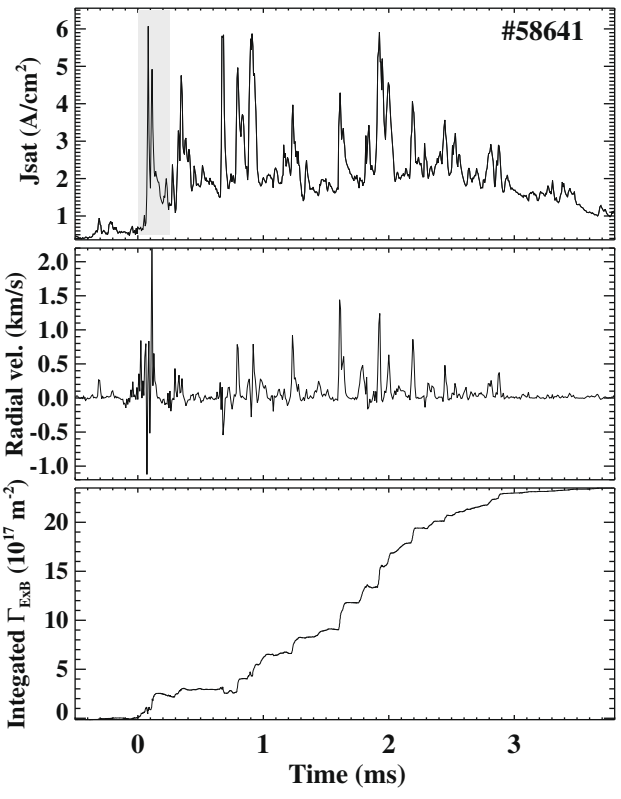

Fig. 1. Time evolution of J_{sat}, v_r and the time integrated $\Gamma_{E\times B}$ during an ELM for a discharge with $I_p = 2$ MA, $B_T = 2.4$ T. The shadowed area indicates the time when the magnetic activity, measured by a B coil in the outer vessel, is significant.

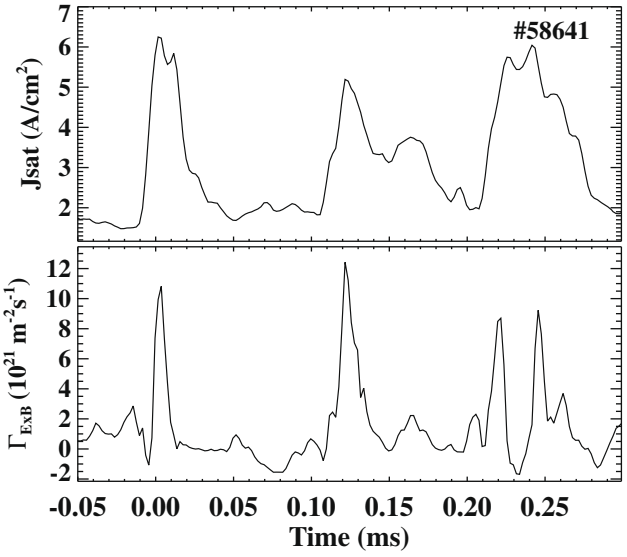

Fig. 2. Time evolution of J_{sat} and $\Gamma_{E\times B}$ during filaments for the some discharge shown in Fig. 1.

typical duration and its averaged J_{sat} and v_r. A clear finding is that the duration of the filaments is larger in L-mode in comparison to that observed during ELMs (see Table 1), while the radial velocity and the density perturbations are smaller. Furthermore, the J_{sat}

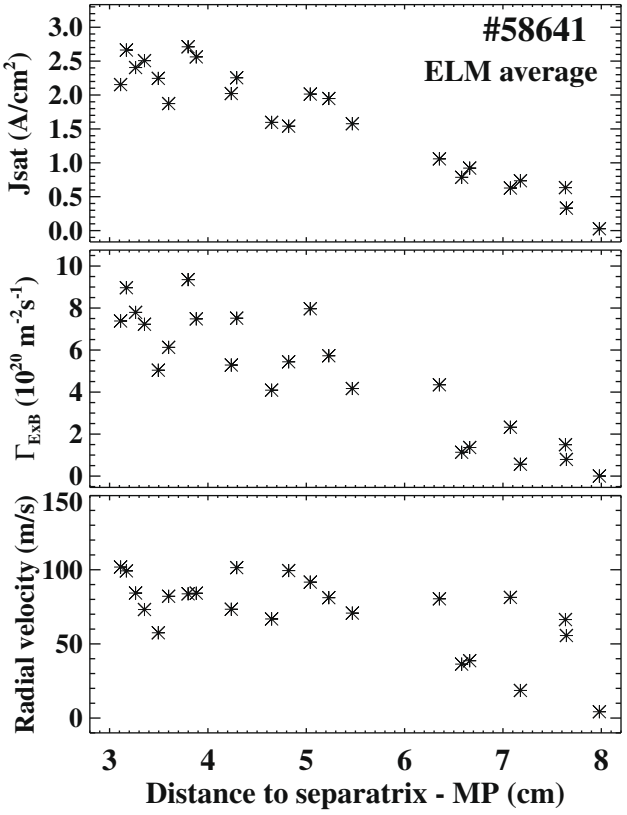

Fig. 3. Radial profile of J_{sat}, $\Gamma_{E\times B}$ and v_r averaged over an ELM for the same discharge shown in Fig. 1.

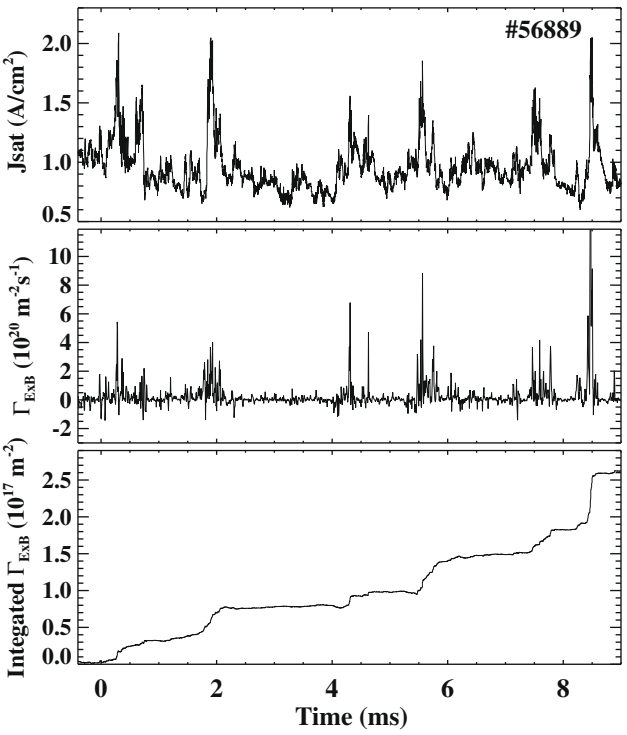

Fig. 4. Time evolution of J_{sat}, v_r and the time integrated $\Gamma_{E\times B}$ for an L-mode discharge with I_p = 1.9 MA, B_T = 1.9 T.

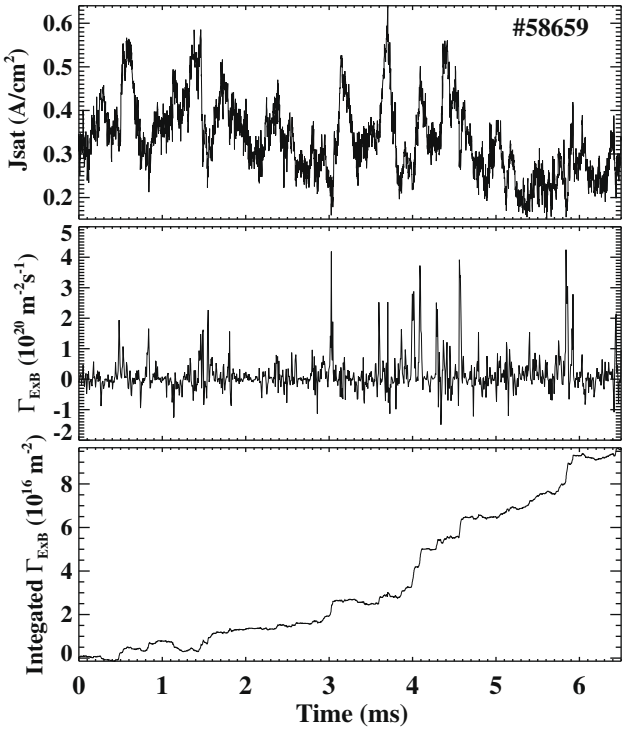

Fig. 5. Time evolution of J_{sat}, v_r and the time integrated $\Gamma_{E\times B}$ in the inter-ELM phase of a discharge with I_p = 1.5 MA, B_T = 3.0 T.

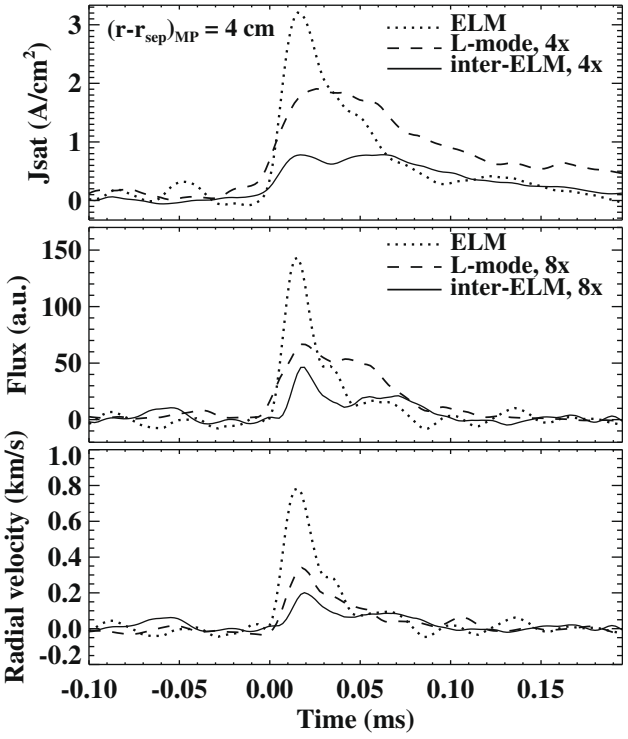

Fig. 6. Conditional average results of J_{sat}, v_r and the time integrated $\Gamma_{E\times B}$ during small ELMs, L-mode and in between ELMs. The J_{sat} ($\Gamma_{E\times B}$) values in L-mode and in the inter-ELM phase are multiplied by 8 (4) to facilitate the comparison between curves.

Table 1
Summary of the intermittent events properties.

	Δt (μs)	J_{sat} (A/cm^2)	v_r (m/s)	Δr (cm)	M_r (×1000)	rms(J_{sat}) (A/cm^2)	Fluctuation level	Skewness	Kurtosis
ELM	55	2.1	380	2.1	1.1	0.85	0.35	1.7	4.6
L-mode	110	0.35	95	1.0	0.4	0.25	0.1	1.9	4.1
Inter-ELMs	130	0.15	60	0.8	0.2	0.08	0.21	0.7	0.5

perturbation during filaments has a stronger dependence on the confinement regime ($J_{sat}^{ELM}/J_{sat}^{inter\text{-}ELM} \approx 14$) than that of v_r ($v_r^{ELM}/v_r^{inter\text{-}ELM} \approx 6$). Using the parameters in Table 1, the radial extension of the filaments ($\Delta r = \Delta t \times v_r$) at $r - r_{sep} \approx 4$ cm is estimated to be ~2 cm during small ELMs, ~1 cm in L-mode and ~0.8 cm in between ELMs, confirming that filaments are radially localized. The value of the filament size in the JET far-SOL predicted by the plasmoid model described in Ref. [12] is in the range of 1–5 cm for Type I ELMs. Taking into account that we have analysed here only small ELMs a reasonable agreement is found.

Probe data has also been analysed to characterize the statistical properties of the J_{sat} intermittency. The root mean square (rms), fluctuations level (rms$[J_{sat}]/\bar{J}_{sat}$), skewness and the kurtosis have been calculated for the different confinement regimes with the same data used for the conditional averaging. As shown in Table 1, a large positive skewness and kurtosis is found in the SOL ($r - r_{sep} \approx 4$ cm) during ELMs and in L-mode confirming the intermittent character of the J_{sat} fluctuations. In spite of the lower magnitude, fluctuations in L-mode have similar statistical properties to those observed during ELMs. On the contrary, fluctuations in the inter-ELM phase, apart from having small amplitude, have a distribution much closer to Gaussian, being therefore less intermittent. As illustrated in Fig. 5, in the inter-ELM phase the magnitude of the filaments is not significantly larger than that of the high frequency background fluctuations characterized by a distribution close to Gaussian [4].

The experimental values shown in Table 1 have also been used to validate theories for the plasma filaments propagation. According to the sheath-detached limit of the interchange theory, the radial Mach number ($M_r = v_r/c_s$) of the filaments should scale as $M_r \propto (\Delta p/p \times \Delta r/R)^{1/2}$, where p is the plasma pressure and Δr the filament size [13]. The pressure has been approximated by J_{sat} as $J_{sat} \propto nT^{1/2}$. Using the experimental values presented in Table 1 and assuming that filaments originate in the pedestal, the radial Mach number of the filaments during ELMs and in L-mode was found to scale with $(\mathrm{rms}(J_{sat})/\bar{J}_{sat} \times \Delta r)^{0.4}$. JET far-SOL results support therefore the sheath-detached filament model as opposed to the model including sheath dissipation that predicts a M_r scaling with $(\Delta r)^{-2}$.

3. Conclusions

SOL parameters measured by the reciprocating probe clearly shows that both Types I and III ELMs are composed of a number of coherent structures or filaments. These structures propagate radially with velocities up to 1 km/s (estimated from the $E_\theta \times B$ turbulent transport flux) with lifetimes in the range 40–100 μs (as seen by the probe ion saturation current). Radial transport in the far-SOL is not continuous but occurs in short bursts observed most often at the beginning of each structure. Furthermore, a sub-structure inside each individual filament is observed, being often a double-peaked structure observed (both in density and turbulent flux). The amplitude of the parallel ion flux during the filaments quickly decreases with radius contrary to the trend observed for the radial velocity which has a weak radial dependence.

Data from the JET boundary plasma have been analyzed to characterize the properties of the intermittent events and to obtain quantitative information on the size, duration and velocity associated with plasma structures for different confinement regimes. It has been found that the duration of the filaments are larger in L-mode when compared to that observed during ELMs while the radial velocity and the density perturbations are smaller. Finally, the J_{sat} fluctuations during ELMs and in L-mode exhibit a large deviation from Gaussian distribution, contrary to the observed in the inter-ELM phase.

Acknowledgements

This work, supported by the European Communities and 'Instituto Superior Técnico' under the Contract of Association between EURATOM and IST, has been carried out within the framework of the European Fusion Development Agreement. Financial support was also received from 'Fundação para a Ciência e Tecnologia' in the frame of the Contract of Associated Laboratory.

References

[1] G.Y. Antar, Phys. Plasmas 10 (2003) 3629.
[2] J.A. Boedo et al., Phys. Plasmas 8 (2001) 4826.
[3] E. Sanchez, C. Hidalgo, D. Lopez-Bruna, I. Garcia-Cortes, R. Balbin, Phys. Plasmas 7 (2000) 1408.
[4] B.A. Carreras, B. Van Milligen, C. Hidalgo, R. Balbin, E. Sanchez, I. Garcia-Cortes, M.A. Pedrosa, J. Bleuel, M. Endler, Phys. Rev. Lett. 83 (1999) 3653.
[5] O E Garcia, J. Horacek, R.A. Pitts, et al., Plasma Phys. Control. Fusion 48 (2006) L1.
[6] C. Silva et al., J. Nucl. Mater. 337–339 (2005) 22.
[7] R.A. Pitts et al., Nucl. Fusion 47 (2007) 1437.
[8] J.A. Boedo et al., Phys. Plasmas 12 (2005) 072516.
[9] W. Fundamenski, R.A. Pitts, Plasma Phys. Control. Fusion 48 (2006) 109.
[10] M. Endler et al., Plasma Phys. Control. Fusion 47 (2005) 219.
[11] J.A. Alonso et al., in: Proceedings of the 34th EPS Conference on Control, Fusion and Plasma Physics, ECA, Warsaw, Poland, 2007.
[12] W. Fundamenski, W. Sailer, Plasma Phys. Control. Fusion 46 (2004) 233.
[13] O.E. Garcia, N.H. Bian, W. Fundamenski, Phys. Plasmas 13 (2006) 082309.